Predicting Scaling Properties from a Single Fluid Configuration

Thomas B. Schrøder[*]

Glass and Time, IMFUFA, Department of Science and Environment, Roskilde University, P.O. Box 260, DK-4000 Roskilde, Denmark

Time-dependent dynamical properties of a fluid cannot be estimated directly from a single configuration without performing a simulation. Here, however, we present a method that predicts the scaling properties of both structure and dynamics from a single configuration. The method is demonstrated to work well for the Lennard-Jones fluid as well as the viscous Kob-Andersen Lennard-Jones mixture, both in and out of equilibrium. The method is conceptually simple and easy to implement and, thus, should become a standard tool in the study of scaling properties of fluids and liquids.

How much can a single configuration tell us about the fluid under the conditions from which it was taken? To be specific, consider the positions of N particles in three dimensions stored in a $3N$-dimensional vector, $\mathbf{R} \equiv (\mathbf{r}_1, \mathbf{r}_2, ..., \mathbf{r}_N)$, where $\mathbf{r}_i$ is the position of the ith particle. Obviously, measures of the structure, such as the radial distribution function, can be estimated from a single configuration, $\mathbf{R}$, with a precision that depends on N. Assuming knowledge of the Hamiltonian, thermodynamic properties such as potential energy and pressure can also be estimated with a per-particle error proportional to $1/\sqrt{N}$. On the other hand, time-dependent dynamical properties such as the mean-square displacement (MSD) and intermediate scattering function can not be directly estimated from a single configuration (some theoretical approaches aim to predict the dynamics from the structure, see, e.g., [1]). This Letter demonstrates that the scaling properties of both structure and dynamics can be easily predicted from a single configuration.

Scaling relations play an important role in physics. Rosenfeld's excess entropy scaling [2–7] states that transport coefficients of fluids depend only on the excess entropy, $S_{ex} \equiv S - S_{ideal}$ (S_{ideal} being the entropy of the ideal gas at the same density and temperature). Another scaling principle is the so-called power-law density scaling, stating that relaxation time and viscosity depend on temperature, T, and density, ρ, only via the combination ρ^{γ}/T, where γ is a material-dependent scaling exponent [8–12] (for a more general scaling principle, see Refs. [13,14]). The scaling requires the use of so-called reduced units, where the unit of energy is given by $e_0 \equiv k_B T$, the unit of length is given by $l_0 \equiv \rho^{-1/3}$, and the unit of time is given by $t_0 \equiv \rho^{-1/3}\sqrt{m/k_B T}$, where m is a characteristic mass of the particles. The described scaling properties—including that they do not always work—are all explained by the isomorph theory [15–17], which we will return to below.

Given a well working scaling relation, one can, from a reference state point, predict the behavior at other state points along the path in the phase diagram characterized by the same value of the scaling variable. We will focus on this aspect, here, by posing the question: How can the dynamics in reduced units be the same at two different state points (ρ_1, T_1) and (ρ_2, T_2)? The simplest explanation is that it is the same differential equation governing the dynamics at the two state points [6]. Restricting ourselves to classical dynamics, Newton's second law can be written, $\mathbf{F}(\mathbf{R}) = \mathbf{m} d^2\mathbf{R}/dt^2$, where $\mathbf{F}(\mathbf{R})$ is the $3N$ dimensional vector containing the forces on the particles, and $\mathbf{m}$ is a diagonal matrix containing the relevant masses. Denoting reduced quantities by a tilde, the reduced force is given by: $\tilde{\mathbf{F}} = \mathbf{F}/(e_0/l_0) = \mathbf{F}/(\rho^{1/3}k_B T)$, and Newton's second law becomes $\tilde{\mathbf{F}}(\mathbf{R}) = \tilde{\mathbf{m}} d^2\tilde{\mathbf{R}}/d\tilde{t}^2$. Thus, if the reduced force depends only on the reduced coordinates, then it is the same differential equation governing the dynamics at the two state points. This will result in the same trajectory in reduced units $\tilde{\mathbf{R}}(\tilde{t})$ [6] and, thus, the same reduced-unit mean-square displacement and intermediate scattering function, as well as the same reduced-unit structure.

The proposed method works as follows. Given a configuration $\mathbf{R}_1$ with density ρ_1 and temperature T_1, we perform an affine scaling to density ρ_2, so that $\rho_2^{1/3}\mathbf{R}_2 = \rho_1^{1/3}\mathbf{R}_1$, i.e., the two configurations are the same in reduced units, $\tilde{\mathbf{R}}_2 = \tilde{\mathbf{R}}_1$. Now, our aim is to choose the temperature T_2 so that the reduced forces of $\mathbf{R}_1$ and $\mathbf{R}_2$, denoted $\tilde{\mathbf{F}}_1$ and $\tilde{\mathbf{F}}_2$, respectively, are as similar as possible. To this end, we define an error function

$$Y \equiv \frac{(\tilde{\mathbf{F}}_2 - \tilde{\mathbf{F}}_1)^2}{\tilde{\mathbf{F}}_1^2 + \tilde{\mathbf{F}}_2^2} = 1 - 2\frac{\tilde{\mathbf{F}}_2 \cdot \tilde{\mathbf{F}}_1}{\tilde{\mathbf{F}}_1^2 + \tilde{\mathbf{F}}_2^2}. \quad (1)$$

Taking the derivative of Eq. (1) with respect to T_2 (which enters via the reduced units in $\tilde{\mathbf{F}}_2$), we find, after straightforward manipulations, that the minimum is located at
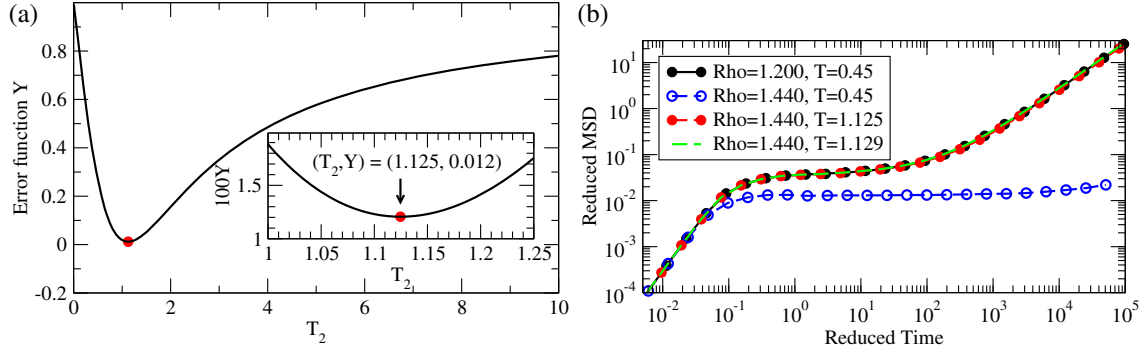
FIG. 1. (a) Error function, Y [Eq. (1)], for a single configuration of the Kob-Andersen binary LJ mixture. The configuration was taken from an equilibrium NVT ($N = 10\,000$) simulation at $(\rho_1, T_1) = (1.20, 0.450)$. Density was increased 20%: $\rho_2 = 1.44$. Inset: enlargement of minimum, note the scale. Red point: Position of minimum, as calculated by Eqs. (2) and (3). (b) Testing the predicted invariance of dynamics: mean-square displacement of large particles in reduced units. The reduced dynamics at $(\rho_2, T_2) = (1.44, 1.125)$ is very close to that of the reference state point, $(\rho_1, T_1) = (1.20, 0.45)$. In contrast, the same density increase on the isotherm, $(\rho, T) = (1.44, 0.45)$, brings the system to a nonequilibrium glass phase, where particles hardly move beyond "cage rattling." Dynamics at $(\rho, T) = (1.44, 1.129)$ is shown as green dashed line.

$$T_2 = \left(\frac{\rho_1}{\rho_2}\right)^{1/3} \frac{|\mathbf{F}_2|}{|\mathbf{F}_1|} T_1, \qquad (2)$$

corresponding to choosing T_2 so that the length of the two reduced force vectors are the same, $|\tilde{\mathbf{F}}_1| = |\tilde{\mathbf{F}}_2|$. The value of the error function at the minimum is

$$Y = 1 - R_{FF}, \qquad R_{FF} \equiv \frac{\mathbf{F}_2 \cdot \mathbf{F}_1}{|\mathbf{F}_2||\mathbf{F}_1|} = \frac{\tilde{\mathbf{F}}_2 \cdot \tilde{\mathbf{F}}_1}{|\tilde{\mathbf{F}}_2||\tilde{\mathbf{F}}_1|}. \qquad (3)$$

where R_{FF} is the Pearson correlation coefficient of the force components, giving the cosine of the angle between $\mathbf{F}_1$ and $\mathbf{F}_2$ (and between $\tilde{\mathbf{F}}_1$ and $\tilde{\mathbf{F}}_2$).

In the following, the method is applied to the $80\!:\!20$ Kob-Andersen binary Lennard-Jones (LJ) mixture [18], a standard model in simulations of viscous liquids. NVT simulations using a Nose-Hoover thermostat with $N = 10\,000$ particles were performed using RUMD [19], an open source molecular dynamics package optimized for GPU computing.

Figure 1(a) shows the error function, Eq. (1), evaluated for a single configuration taken from an equilibrium simulation at $(\rho_1, T_1) = (1.20, 0.45)$. A 20% increase in density was applied. The minimum is given by $T_2 = 1.125$ [Eq. (2)], and $Y = 0.012$ [Eq. (3)] corresponding to a Pearson correlation coefficient $R_{FF} = 0.988$.

The predicted invariance of the dynamics is tested in Fig. 1(b). Results for the reference state point $(\rho_1, T_1) = (1.20, 0.45)$ (filled black circles) shows a plateau in the mean square displacement as is characteristic for viscous liquids. The reduced dynamics at $(\rho_2, T_2) = (1.44, 1.125)$ (red filled circles) is, to a very good approximation, the same as at the reference state point. From this, we conclude that the method works very well: from a single configuration, we predicted a new state point at which the reduced

dynamics is indistinguishable from that of the reference state point. The corresponding invariance of the intermediate scattering function and structure is shown in the Supplemental Material [20], Figs. S1 and S2.

What if we had chosen a different configuration to apply the method to? Applying the method to 178 independent configurations gives a mean $T_2 = 1.1249$ with a standard deviation 0.0014 (distribution shown in the Supplemental Material [20], Fig. S3). Because of the strong temperature dependence of viscous liquids, we tested whether picking a configuration from the tail of this distribution, $T_2 = 1.129$, alters the conclusion; the green dashed line in Fig. 1(b) shows that this is not the case.

Can the new method predict whether the scaling will work or not? A necessary requirement is that the force components before and after scaling are strongly correlated, i.e., that $\mathbf{F}_1$ and $\mathbf{F}_2$ are close to being parallel, and thus, $\tilde{\mathbf{F}}_1 \approx \tilde{\mathbf{F}}_2$. Figure 2(a) shows a scatter plot of the force components before and after scaling for a low density state point where scaling does not apply (see Supplemental Material [20], Fig. S4). The inset reveals that a subset of small force components is correlated with a smaller slope, a feature that is not present for the high density state point where scaling works, see Fig. 2(b). This difference does not lead to significantly different Pearson correlation coefficients (0.983 and 0.988). Thus, a Pearson coefficient close to unity, and thereby an error function, Y, close to zero [Eq. (3)] is a necessary, but not sufficient condition for the method to work. In contrast, the Spearman correlation coefficient [the Pearson correlation coefficient of the rank of the data, see Supplemental Material [20], Fig. S5], is different for the two cases: 0.836 and 0.985, respectively. More tests are needed, but a criterion for expecting the scaling to work might be that both the Pearson and Spearman correlation coefficients should be larger than 0.95.
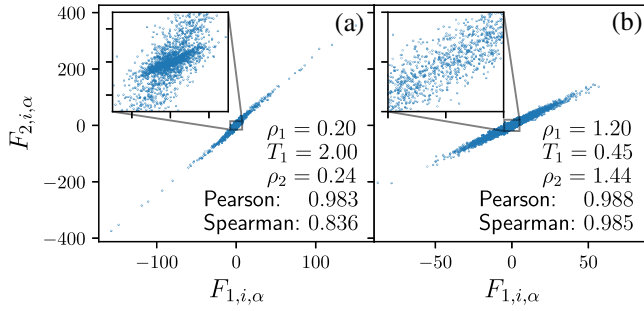
FIG. 2. Force components, $F_{2,i,\alpha}$, of a single scaled configuration versus force components, $F_{1,i,\alpha}$, of the same configuration before scaling. 10% of data points displayed. (a) Low density state point where scaling does not apply. (b) High density state point where scaling does apply.

We conclude from the results presented above that when the scaling works, the two state points are, indeed, characterized by reduced forces that, to a good approximation, depend only on the reduced coordinates. The simplest explanation for this is that the relevant part of the reduced potential energy surface is the same, except for an additive constant

$$\frac{U(\mathbf{R}_2)}{k_B T_2} = \frac{U(\mathbf{R}_1)}{k_B T_1} + C, \qquad \rho_2^{1/3}\mathbf{R}_2 = \rho_1^{1/3}\mathbf{R}_1. \quad (4)$$

This is the fundamental assumption of the isomorph theory [15] (for a more general formulation, see Ref. [17]). Taking the gradient on both sides of Eq. (4) leads to the reduced forces being the same for the two state points. This, in turn leads to the reduced dynamics and structure being the same, which in turn, also leads to excess entropy, S_{ex}, being the same [15]. "Isomorphs" are curves in the phase diagram where any two state points fulfill Eq. (4) to a good approximation and, thus, are characterized by approximately invariant reduced-unit structure, dynamics, and excess entropy.

In the context of the isomorph theory, the force-based method presented here is a new method for identifying isomorphs. For comparison, we will briefly describe the two most used existing methods, the γ method and the direct isomorph check.

In the γ method, a curve in the phase diagram with constant S_{ex}, i.e., a configurational adiabat, is traced out using the general statistical mechanics identity [15]

$$\gamma \equiv \left(\frac{\partial \ln T}{\partial \ln \rho}\right)_{S_{\text{ex}}} = \frac{\langle \Delta W \Delta U \rangle}{\langle (\Delta U)^2 \rangle} \quad (5)$$

where $\langle \ldots \rangle$ denotes canonical (NVT) ensemble average, and Δ denotes deviation from the ensemble average. The right hand side of this equation is evaluated from equilibrium NVT simulations, and the configurational adiabat is traced out by numerically solving the differential equation,

Eq. (5). The main disadvantage of this method is that it requires small steps in density, which can pose a practical problem in particular in viscous liquids where long simulations are needed to accurately evaluate the right hand side.

Equation (4) can be rewritten as: $U(\mathbf{R}_2) = (T_2/T_1)U(\mathbf{R}_1) + D$. This is the basis of the direct isomorph check [15]: (i) an equilibrium NVT simulation is performed at a state point (ρ_1, T_1); (ii) a number of configurations are scaled affinely to a new density ρ_2 [$\mathbf{R}_2 = (\rho_1/\rho_2)^{1/3}\mathbf{R}_1$]; (iii) the potential energy of the scaled configurations, $U(\mathbf{R}_2)$, is plotted against the potential energy of the unscaled configurations, $U(\mathbf{R}_1)$ in a scatter plot; (iv) for the isomorph theory to apply $U(\mathbf{R}_2)$ and $U(\mathbf{R}_1)$ need to be strongly correlated, in which case the new temperature can be determined from the slope being equal to T_2/T_1. The main advantage of this method is that large density changes can be performed from a single equilibrium NVT simulation. For Lennard-Jones type systems, the direct isomorph check can be performed analytically [16]

$$\frac{T_2}{T_1} = \left(\frac{\rho_2}{\rho_1}\right)^4 \left(\frac{\gamma_1}{2} - 1\right) - \left(\frac{\rho_2}{\rho_1}\right)^2 \left(\frac{\gamma_1}{2} - 2\right), \quad (6)$$

where γ_1 is Eq. (5) evaluated at the reference state point.

In Fig. 3(a), the new force-based method [Eq. (2)] is compared to the analytical direct isomorph check [ADIC, Eq. (6)], using the same reference point as in Fig. 1, varying ρ_2 from 1.26 to 1.60. The new method clearly outperforms the direct isomorph check.

In Fig. 3(b), it is shown how to apply the new method to collapse data covering a broad region of the phase diagram. In the inset, the reduced diffusion coefficient is plotted as a function of temperature, T_1, for different isochores with density ρ_1. The spread in the data illustrates the well-known strong state-point dependence of the dynamics of viscous liquids. Now, we choose $\rho_2 = 1.6$, and, for each state point (ρ_1, T_1), scale a single configuration to ρ_2 and use Eq. (2) to compute the corresponding value of T_2. For each ρ_1 isochore, this gives a prediction for the dynamics on the ρ_2 isochore. If the method is working correctly, these predictions should all agree with the $\rho_1 = 1.6$ isochore, i.e., the data should collapse on a single curve. The main panel of Fig. 3(b) shows that this works very well [note, however, that deviations of around 10% as observed in Fig. 3(a) are not visible when plotting data as in Fig. 3(b)].

In Fig. 4, the force method is tested for the nonviscous single component Lennard-Jones system over a broad range of densities. At high initial densities, where the Spearmann coefficient is high, the force-based method traces out paths in the phase diagram along which the reduced diffusion coefficient is relatively invariant. At low initial densities, where the Spearmann coefficient is low (e.g., $\rho_1 = 0.2$), the reduced diffusion coefficient is also
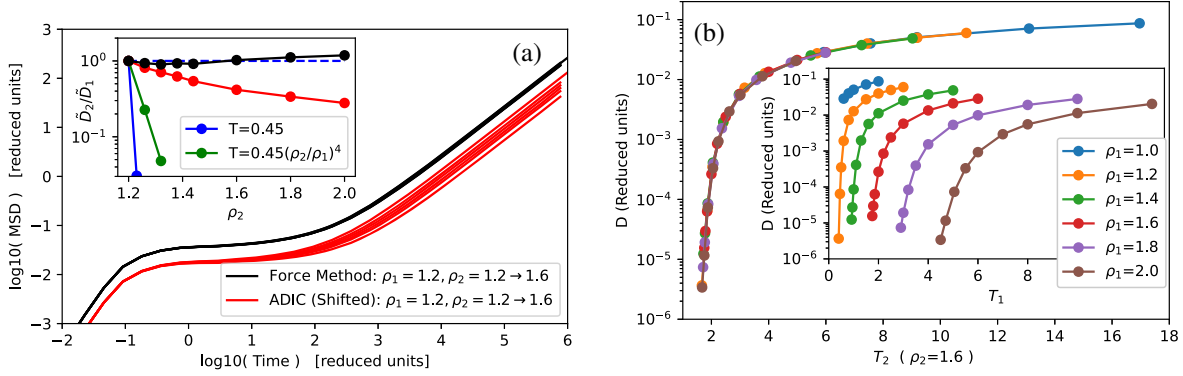
FIG. 3. (a) Mean-square displacement in reduced units along two paths in the phase-diagram with densities $\rho_2 = 1.20, 1.26, 1, 32,$ 1.38, 1.44, 1.60. Black curves: the force based method [Eq. (2)] using a single equilibrium configuration from the reference state point, $(\rho_1, T_1) = (1.20, 0.45)$. Red curves: analytical direct isomorph check [ADIC, Eq. (6), shifted 0.5 down]. Here, $\gamma_1 = 5.167$ was calculated from an equilibrium simulation with a duration of approximately 1000 times the alpha relation time at the reference state point. Inset: Reduced diffusion coefficients relative to the reference state point. Included for comparison: isotherm (blue) and the scaling expected from the repulsive r^{-12} term in the LJ potential (green). (b) Inset: reduced diffusion coefficient as a function of temperature, T_1, for six isochores. Main panel: Same reduced diffusion coefficients, plotted as function of T_2 as given by Eq. (2) with $\rho_2 = 1.6$.

relatively invariant, but we note that this is not the case for the reduced structure (see Supplemental Material [20], Fig. S7). For this system, the force-based method performs slightly worse than the direct isomorph check at high densities (compare, e.g., Supplemental Material [20], Fig. S6). Thus, which method works best depends on the system and the state point. The methods are uncontrolled approximations; they can be derived from assuming Eq. (4) is exact, but presently, we can not predict the magnitude of the error in, e.g., the reduced diffusion coefficient when this is not the case. Consequently, presently, we can not predict which method performs best in a given situation beforehand.

The new force based method can be applied to a single configuration, which does not have to be from a constant volume simulation, nor does it have to be in equilibrium. In the following, we will showcase an application illustrating the last two points—to our knowledge, no other method has these possibilities.

When a glass-forming liquid is cooled continuously, it eventually falls out of equilibrium and forms a glass. In Fig. 5, the black circles shows the density of the Kob-Andersen mixture as a function of temperature during continuous cooling at pressure $P = 10$ (MD units). To be specific, it is the density of individual configurations visited during the cooling that is plotted. This leads to some scatter in the data, but a glass transition around $T_g \approx 0.6$ is still clearly observed from the change of slope.
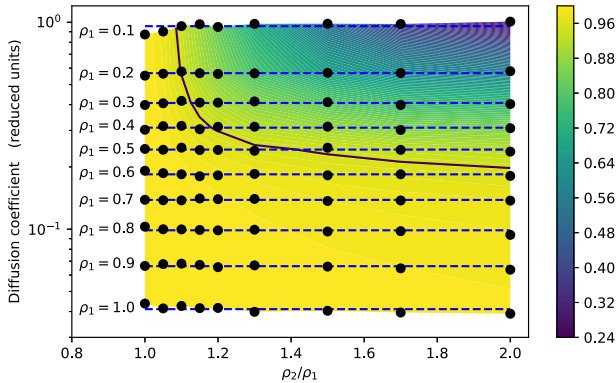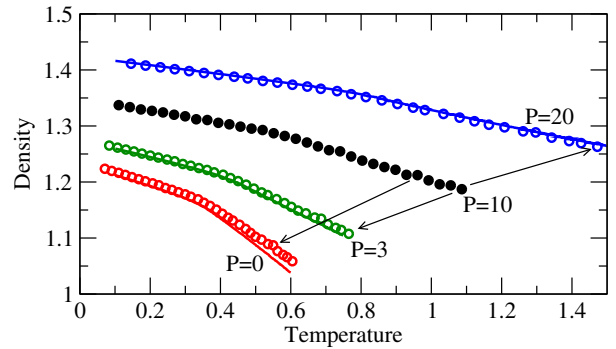

FIG. 4. Reduced-unit diffusion coefficients along ten different paths in the phase diagram of the single component LJ system ($N = 4000$). Each path is generated using Eq. (2) by scaling a single configuration from a reference state point, $(\rho_1, T_1 = 2.0)$. ρ_1 varies from 0.1 to 1.0 (close to the freezing line [21]). Blue dashed lines give the mean value of the reduced diffusion coefficients for the given path. Color map quantifies the Spearman correlation coefficient of force components before and after scaling, with the black curve identifying the value 0.95.

FIG. 5. Density, ρ, versus temperature, T, for isobaric cooling curves of the Kob-Andersen mixture. Predictions for cooling curves at $P = 20$, 3, and 0 (blue, green, and red open circles) were calculated from the $P = 10$ cooling curve (filled black circles), as described in the text. Good agreement is found with actual simulated cooling curves (blue, green, and red lines). The same cooling rate ($dT/dt = -2.0 \times 10^{-6}$) was used in all cases. Adjusting cooling rates to be isomorphic has minimal influence on the results (Supplemental Material [20], Fig. S8).

From the $P = 10$ cooling curve, the "isomorphic" cooling curve for $P = 20$ can be predicted. For each of the stored $P = 10$ configurations (black circles in Fig. 5), the corresponding isomorphic configuration at $P = 20$ is found as follows. The $P = 10$ configuration is scaled to a higher density, the isomorphic temperature, T_2, is evaluated from Eq. (2), and the pressure is evaluated from $P = \rho_2 k_B T_2 + \rho_2 W_2/N$, where W_2 is the virial of the scaled configuration. This procedure is repeated, adjusting the density until the desired pressure $P = 20$ is achieved with satisfactory precision. The resulting (T, ρ) pairs are plotted as blue circles in Fig. 5. Corresponding results for $P = 3$ and $P = 0$ are shown in green and red, respectively. Actual simulated cooling curves initiated from equilibrated samples at $(P, T) = (20, 1.5), (3, 0.8), (0, 0.6)$, are plotted as full lines. Deviations are seen at the lowest pressure $P = 0$, but in general, quite good agreement is observed between the actual simulated cooling curves and the predicted cooling curves. This confirms that the force method can, indeed, be used without constant volume, and out of equilibrium, as argued above.

To summarize, we have presented an easily applicable method to predict scaling properties of fluids. The method was demonstrated to work very well in several applications, leading to the intriguing consequence that information about scaling properties is contained in individual configurations. This is in stark contrast, e.g., to Rosenfeld's excess entropy scaling [2,3,6], where the excess entropy usually is calculated by thermodynamic integration, requiring equilibrium data along paths in the phase diagram. A further feature of the new method is that it does not require constant volume nor equilibrium conditions, in contrast to existing methods. Further testing of the method is needed, in particular, for molecular systems. Since the method utilizes a key feature of the isomorph theory (the invariance of reduced forces), the expectation is that the method is applicable for the many systems where the isomorph theory has been found to work well. This includes systems where the interactions are dominated by van der Waals or weakly ionic and dipolar interactions, as well as metals, but excludes systems dominated by directional bonds or strong Coulomb forces [17]. An open question is why does the method trace out paths of invariant reduced diffusion coefficient at low densities (e.g., $\rho = 0.2$ in the single component LJ system, Fig. 4)? On the one hand, this is not explained by the isomorph theory since the structure is not invariant, on the other hand it is hardly a coincidence. Investigating this question may lead to new insights into the physics of the low-density fluid state.

[*] tbs@ruc.dk

[1] W. Götze, *Complex Dynamics of Glass-Forming Liquids: A Mode-Coupling Theory* (Oxford University Press, New York, 2009).

[2] Y. Rosenfeld, Relation between the transport coefficients and the internal entropy of simple systems, Phys. Rev. A **15**, 2545 (1977).

[3] J. Mittal, J. R. Errington, and T. M. Truskett, Thermodynamics Predicts How Confinement Modifies the Dynamics of the Equilibrium Hard-Sphere Fluid, Phys. Rev. Lett. **96**, 177804 (2006).

[4] R. Chopra, T. M. Truskett, and J. R. Errington, Excess entropy scaling of dynamic quantities for fluids of dumbbell-shaped particles, J. Chem. Phys. **133**, 104506 (2010).

[5] E. H. Abramson, Viscosity of argon to 5 GPa and 673 K, High Press. Res. **31**, 544 (2011).

[6] J. C. Dyre, Perspective: Excess-entropy scaling, J. Chem. Phys. **149**, 210901 (2018).

[7] I. H. Bell, J. C. Dyre, and T. S. Ingebrigtsen, Excess-entropy scaling in supercooled binary mixtures, Nat. Commun. **11**, 4300 (2020).

[8] A. Tölle, Neutron scattering studies of the model glass former ortho-terphenyl, Rep. Prog. Phys. **64**, 1473 (2001).

[9] C. M. Roland, S. Hensel-Bielowka, M. Paluch, and R. Casalini, Supercooled dynamics of glass-forming liquids and polymers under hydrostatic pressure, Rep. Prog. Phys. **68**, 1405 (2005).

[10] D. Coslovich and C. M. Roland, Pressure-energy correlations and thermodynamic scaling in viscous Lennard-Jones liquids, J. Chem. Phys. **130**, 014508 (2009).

[11] T. B. Schrøder, U. R. Pedersen, N. P. Bailey, S. Toxvaerd, and J. C. Dyre, Hidden scale invariance in molecular van der Waals liquids: A simulation study, Phys. Rev. E **80**, 041502 (2009).

[12] D. Fragiadakis and C. M. Roland, On the density scaling of liquid dynamics, J. Chem. Phys. **134**, 044504 (2011).

[13] C. Alba-Simionesco, D. Kivelson, and G. Tarjus, Temperature, density, and pressure dependence of relaxation times in supercooled liquids, J. Chem. Phys. **116**, 5033 (2002).

[14] C. Alba-Simionesco and G. Tarjus, Temperature versus density effects in glassforming liquids and polymers: A scaling hypothesis and its consequences, J. Non-Cryst. Solids **352**, 4888 (2006), Proceedings of the 5th International Discussion Meeting on Relaxations in Complex Systems.

[15] N. Gnan, T. B. Schrøder, U. R. Pedersen, N. P. Bailey, and J. C. Dyre, Pressure-energy correlations in liquids. IV. "Isomorphs" in liquid phase diagrams, J. Chem. Phys. **131**, 234504 (2009).

[16] L. Bøhling, T. S. Ingebrigtsen, A. Grzybowski, M. Paluch, J. C. Dyre, and T. B. Schrøder, Scaling of viscous dynamics in simple liquids: Theory, simulation and experiment, New J. Phys. **14**, 113035 (2012).

[17] T. B. Schrøder and J. C. Dyre, Simplicity of condensed matter at its core: Generic definition of a Roskilde-simple system, J. Chem. Phys. **141**, 204502 (2014).

[18] W. Kob and H. C. Andersen, Scaling Behavior in the β-Relaxation Regime of a Supercooled Lennard-Jones Mixture, Phys. Rev. Lett. **73**, 1376 (1994).

[19] N. P. Bailey, T. S. Ingebrigtsen, J. S. Hansen, A. A. Veldhorst, L. Bøhling, C. A. Lemarchand, A. E. Olsen, A. K. Bacher, L. Costigliola, U. R. Pedersen, H. Larsen, J. C. Dyre, and T. B. Schrøder, RUMD: A general purpose molecular dynamics package optimized to utilize GPU hardware down to a few thousand particles, SciPost Phys. **3**, 038 (2017).

[20] See Supplemental Material at http://link.aps.org/supplemental/10.1103/PhysRevLett.129.245501 for figures with supplementing simulation results.

[21] U. R. Pedersen, L. Costigliola, N. P. Bailey, T. B. Schrøder, and J. C. Dyre, Thermodynamics of freezing and melting, Nat. Commun. **7**, 12386 (2016).